SAR TOMOGRAPHY AT L BAND APPLIED TO FOREST STRUCTURE ANALYSIS

DANIEL MÁXIMO GARCIA [1]
MARIA TELLO ALONSO [1]

[1] Deutsches Zentrum für Luft- und Raumfahrt e.V. (DLR)
Microwaves and Radar Institute
Münchener Str. 20 - 82234 Weßling - Germany
{daniel.garcia, maria.telloalonso}@dlr.de

Abstract. The upcoming launch, scheduled for the next decade, of the BIOMASS and the TANDEM L space missions will have a special focus on forest applications. However, it is still necessary to research the amount and the quality of information relevant to forest structure parameters that those SAR sensors can possibly retrieve. SAR tomography is an advanced technique capable to measure the three dimensional structure information from forest scenarios. In this direction, this paper confronts the information provided by a series of reflectivity profiles, generated using the techniques of SAR Tomography with the capon inversion algorithm, with a set of terrestrial inventory plots, where the spatial distribution of trees, as well as some of their morphological characteristics, are available. These reflectivity profiles measures the energy backscattered of several points along the height of the forest, from the ground up to the top of the canopy. According to the polarization and the composition of the forest, the signal response may vary widely and some features can be highlighted. As an input it was used a fully polarimetric airborne dataset from DLR’s E-SAR system, four spatial and temporal baselines were employed along with lidar measurements of forest height and topography over the managed forest of Traunstein – Germany.

Key words: SAR tomography, forest structure, capon spectral estimator, tomografia SAR, estrutura florestal, estimador espectral capon.

1. Introduction

In the current context of intense discussion about climate change, there is an increasing interest in monitoring forest dynamics at a global scale. Furthermore, besides the need of global measurements, 3D observables are required in several forest applications, such as biomass estimation, where it has been shown that allometric equations exclusively based on forest heights are not sufficient to produce accurate biomass estimates.

Synthetic Aperture Radar (SAR) signals at low frequencies can penetrate forest. This capability allows, through advanced imaging techniques such as polarimetric interferometric SAR (Cloude and Papathanassiou, 1998) and tomography (Reigber and Moreira, 2000), the extraction of relevant information related to the three dimensional structure of the observed scene. More specifically, in the case of tomography, through repeated passes of the sensor, a scene is observed under slightly different observation angles and this angular diversity can be exploited to retrieve the three dimensional reflectivity signature of the scene. Furthermore, by employing different transmitting and receiving polarizations, the polarimetric behavior of the different scatterers can be discriminated, allowing an enriched characterization of the scene. In the last years, several airborne tomographic SAR experiments at low frequencies have already proven the unprecedented potential of this technique to provide a deep insight on forest structure. Moreover, several SAR space missions are planned to be launched in the next decade (BIOMASS, Tandem-L) with a special focus on forest applications.

However, it is still an open question to fully understand and assess the amount and quality of the information relevant to forest structure that systems based on SAR tomography can retrieve. Hence, the aim of this paper is to address this question through the confrontation of airborne tomographic SAR measurements with terrestrial inventory plots for a number of stands with different structures and species composition.

The remainder of this paper is structured as follows. Section 2 summarizes the theoretical background. Section 3 describes the experimental framework test site and the methodology.

Results are presented in section 4 and some conclusions and discussions are drawn in section 5.

2. Capon SAR tomography: theoretical principles

Consider N different SAR acquisitions of a given region of interest to be imaged. Each acquisition has a baseline distance B_j from the reference track, also called master track. For a given acquisition n, the azimuth-range resolution cell (x, r) contains n_s backscattering contributions from scatters located at different heights, and the complex pixel value after some phase corrections is:

$$g_n = \sum_{z=1}^{n_s} \gamma(z) \exp(-jk_{zn} z) = FT[\gamma(z)]|_{k_{zn}}, \ \mathrm{n} = 1, \ldots, \mathrm{N} \quad (1)$$

Where k_z is the two-way vertical wavenumber between the master and the *n*th acquisition track and $\gamma(x, r, z)$ is the 3D reflection distribution. In other words, the resolution cell of a SAR image is the Fourier Transfer of the reflection function in the elevation direction at the position k_z. Considering the set of N baselines, we define the steering vector a(z) that contains the interferometric phase information associated to a source located at the elevation position z above the reference focusing plane as:

$$a(z) = [1, \exp(jk_{z2} z), ..., \exp(jk_{zN} z)]^T \quad (2)$$

The respective steering matrix A(z) = [a(z_1),…,a(z_{ns})] consists of n_s steering vectors corresponding each to a backscattering source, with z = [z_1,…, z_{ns}]^T being the vector of unknown source heights. As it is explained in details in (Huang et al., 2011), the problem consists of the estimation of the elevation z_i and the reflectivity $\sigma(z) = |\gamma(z)|^2$ of each n_s source, which covariance matrix R is characterized by:

$$R = A(z) P \mathrm{A}^{\dagger}(z) + \sigma_n^2 I_{(NxN)} \quad (3)$$

Where P represents the (n_s x n_s) source signal covariance matrix and $\mathrm{A}^{\dagger}$ is the hermitan matrix. To solve equation (3) an algorithm called Capon (Capon, 1969) was used. The capon method is a non-linear based adaptive (data-dependent) filterbank method. The first rank capon estimated backscattered signal power height spectrum from a N multibase SAR tomography dataset is given by:

$$\widehat{P}_C(z) = [a^H(z) \widehat{R}_y^{-1} a(z)]^{-1} \quad (4)$$

Where $(.)^H$ denotes conjugate transpose, $\widehat{R}_y$ is a multi-look estimate of the array data covariance matrix. As a consequence of an irregular baseline sampling this algorithm is sensitivity to the acquisition configuration. In other words, the capon method has a good resolution but a reduced radiometric accuracy.

3. Forest structure observation with an airborne TomoSAR system

An airborne campaign was carried out by DLR with its E-SAR system over the area of Traunstein in 2009. The Traunstein test site is located in the southwest of Germany. The topography varies from 600 m to 800 m amsl, with only few steep slopes. It is a temperate heterogeneous managed forest composed of even-aged stands, dominated by beeches and spruces with heights ranging from 10 to 40 meters.

E-SAR was flying 4 tracks over the Traunstein forest on the 28th October 2009. The 4 tracks were acquired, with a temporal spacing of a few minutes and spatial baselines between one track and the next one of around 5 meters. The wind speed was low and it was a sunny day, with low humidity. The dataset is fully polarimetric at L-band, the range and the azimuth resolutions are 2.12 and 1.2 meters respectively. LIDAR measurements are also available and are used as a reference for the forest height and the ground topography.

On the other hand, a set of georeferenced inventory plots are available. Each of these inventory plots covers an area of 25 x 25 meters. The number, position, type and dimensions of the trees are measured.

Regarding the processing of the data carried out in the scope of this paper, the topography is first corrected with the LIDAR measurements. For the estimation of the coherences in the covariance matrix, a multilook of 5 pixels in range and 11 pixels in azimuth is applied. The reflectivity profiles are then obtained for each range and azimuth position, for each polarization by means of a rank one Capon inversion. As an example, figure 1 shows for a fixed position in range and along several kilometers in azimuth, the resulting tomogram after topography removal, for different polarizations. The bare soil and the forested areas can be easily identified. Besides, it can be observed that even if in general the highest reflectivity is measured at the top of the canopy, the radar signal at L-band is able to penetrate until the ground since energy is backscattered in the vertical dimension at every height in the forest body, from the ground to the top of the trees. The difference of behavior between the polarizations is also noticeable at first sight. Co-polar channels have a higher backscatter compared to the cross-polar ones and, in particular, the ground is more recognizable at HH and VV.

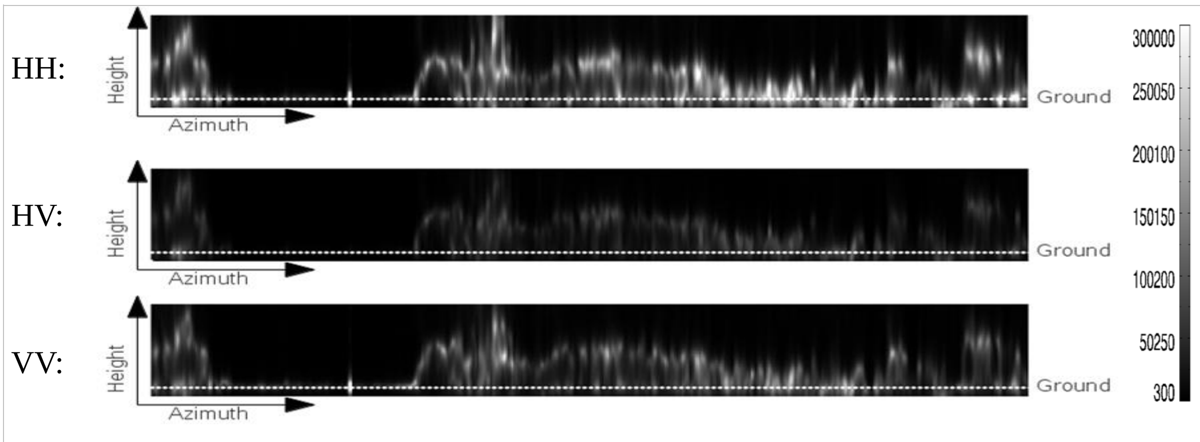

Figure 1. Tomograms of the test site considered at HH (top), HV (center) and VV (bottom) polarizations

4. Results

In order to address the question of the sensitivity of the reflectivity profiles to parameters relevant to forest structure, the tomographic SAR dataset is confronted to terrestrial data in a set of inventory plots. In the scope of this paper, six particular examples are presented and analyzed. It should be noted that an inventory plot covers an area of around 25x25 meters, which corresponds to a window of 3x3 pixels in the SAR dataset. Therefore, for each inventory plot, the 9 corresponding vertical reflectivity profiles are considered and for the results exposed in this paper, superimposed in the same plot. Besides, each reflectivity profile is normalized to the maximum power in the window. Since VV and HH, as well as VH and HV exhibit an analogous behavior, only HH and HV polarizations are shown hereafter.

The first situation considered is the simplest one with one single high tree in the area covered by the inventory plot, see figure 2. Therefore, in this particular case, it is expected that only a limited number of reflectivity profiles intercept the tree. Two analogous examples are analyzed in parallel, where the only difference between them is the type of tree: the tree in figure 2 a) is a beech, whereas the tree in figure 2 b) is a spruce. Since the SAR data was acquired in autumn, it can be assumed that the beech had almost no leaves, unlike the spruce. Consistently with this, we observe in the reflectivity profiles that the tomographic SAR system is almost not sensitive to the presence of the isolated beech: most of the energy is backscattered from the ground, despite a small peak at HV, at around 30 meters. On the other hand, for the spruce, peaks are noticeable in the reflectivity profiles in both HH and HV polarizations at 30 and 25 meters respectively.

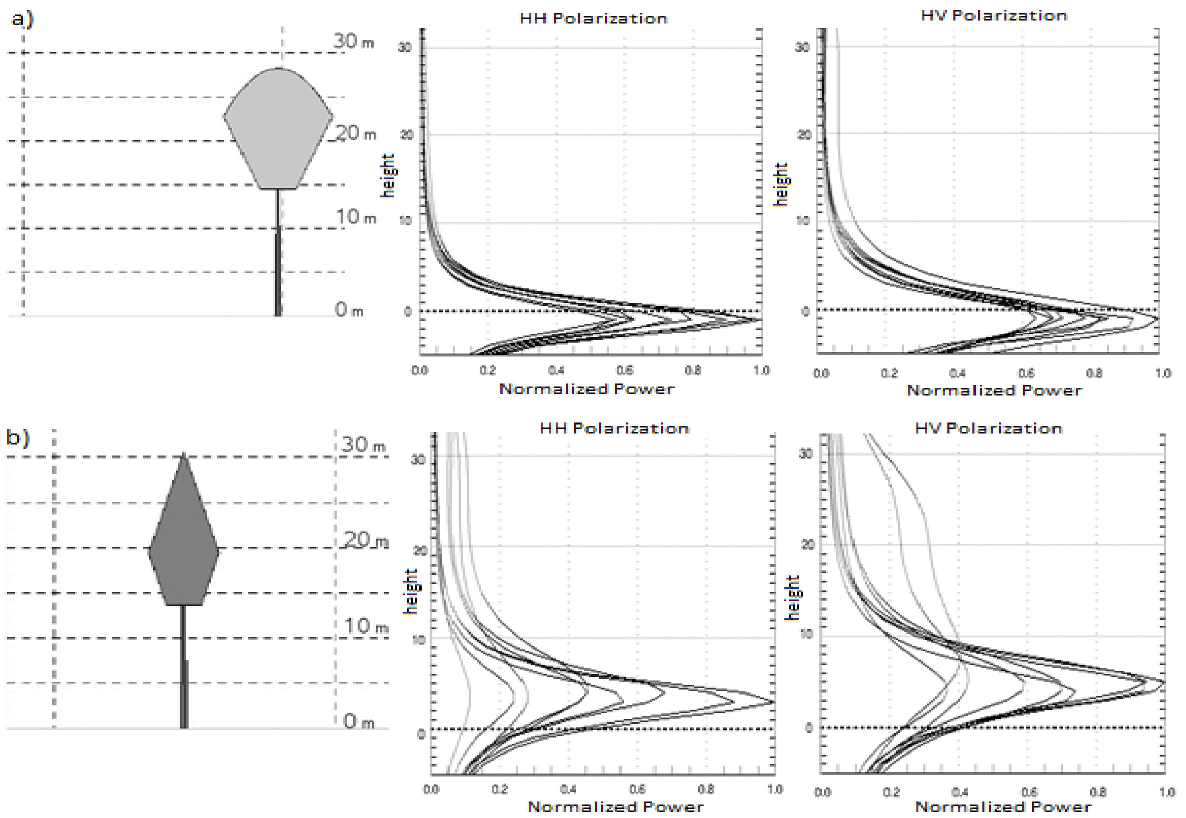

Figure 2. Two examples of inventory plots (left column) and reflectivity profiles at HH (center column) and HV (right column) polarizations, with only one tree, different species: beech (a) and spruce (b).

The second situation analyzed are two homogeneous stands, see figure 3. The first one is entirely constituted by beeches, with heights ranging from 30 to 38 meters (see figure 3 a)) and the second one has only spruces on it, with a similar height of 35 meters (see figure 3b)). In this case, the group of trees is clearly noticeable by the SAR system at the two polarizations considered. For the stand of beeches, the reflectivity profiles at HH have large peaks at ground level, and smaller ones at heights from 20 to 30 meters, corresponding to the center / top of the canopy. The same observation is valid at HV polarization, with the difference that the contribution of the branches is more significant. Besides, five peaks can be observed between 0 and 8 meters. They are produced by the presence of scatterers in the understory. Similar observations are valid for the stand of spruces, despite the lower position of the peak, located at the center of the canopy. Furthermore, at HV polarization the volume scattering contribution by the branches and leaves is more important than in the stand of beeches and, as a consequence, the peak in the ground appears very low with respect to that at the canopy level.

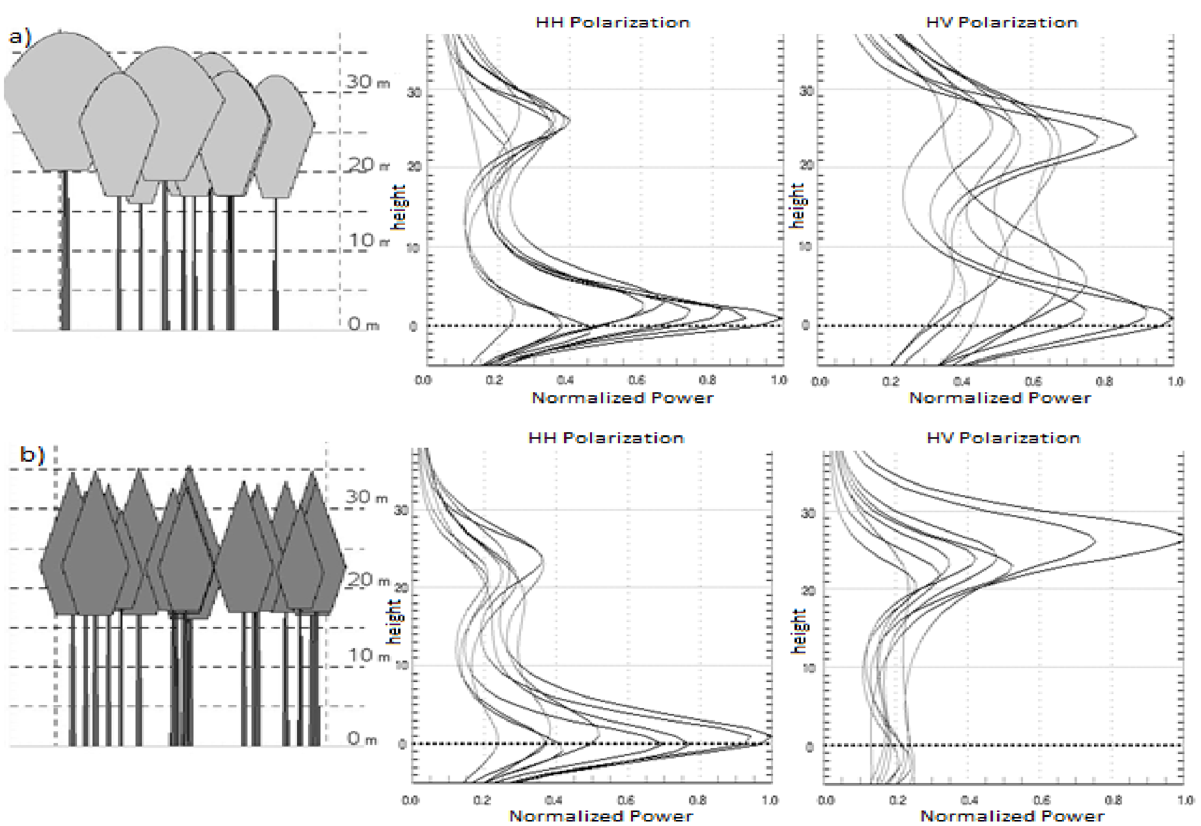

Figure 3. Two examples of inventory plots (left column) and reflectivity profiles at HH (center column) and HV (right column) polarizations, both with homogeneous stands, but different species: beech (a) and spruce (b).

The last set of examples considered corresponds to stands with a rich structure, constituted by different types of trees, unevenly distributed, with distinct heights (see figure 4). In that case, the backscatter from the ground is very low and for both stands and both polarizations considered, the reflectivity profiles exhibit a greater diversity than in the previous situations. The positions of the peaks are more distributed along the vertical dimension. For example, for stand in figure 4 a) at HH polarization, a wide peak can be observed at around 5 m and the other peaks are distributed between 15 and 25 m. An analogous observation is valid for the crosspolar channel. For stand in figure 4 b), at HH polarization, two distinct groups of peaks can be distinguished: one around 10 m, corresponding to the top height of the dense group of small trees and the second one around 20 m. In figure 2 b), most of the energy backscattered by a single spruce occurred at the center of the canopy, i.e. at around 30 m in this case according to the inventory plot. The absence of peaks around 30 m in the reflectivity profiles in figure 4 b) suggests the importance of the interactions between trees in the vertical distribution of the backscattering.

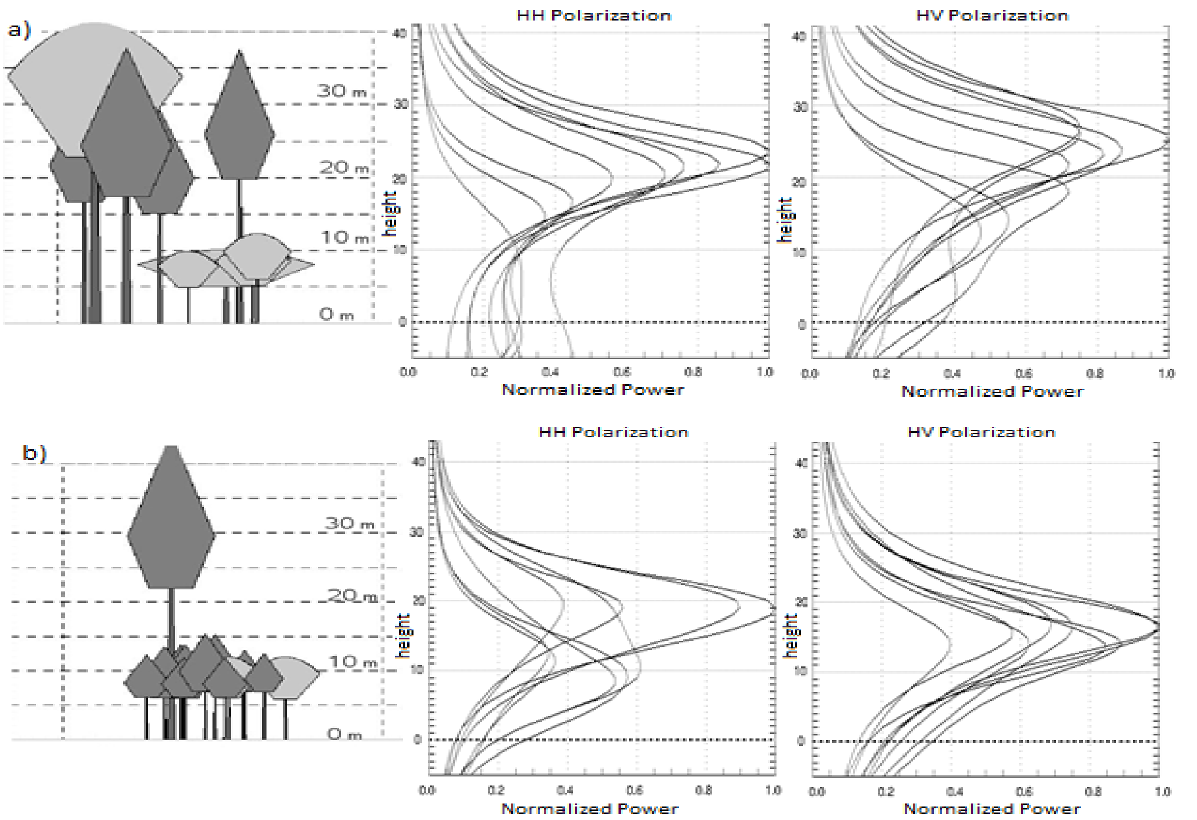

Figure 4. Two examples of inventory plots (left column) and reflectivity profiles at HH (center column) and HV (right column) polarizations, both with heterogeneous stands.

5. Conclusions

This paper opens a discussion about the capabilities of SAR tomography at L-band for forest structure characterization. The results of an airborne campaign in a temperate climate are presented and confronted to terrestrial ground truth data. In particular, a set of inventory plots is analyzed and a sample of them is shown in this work.

According to the results obtained, it is proven than SAR tomography at L-band can penetrate the forest body, reaching the ground level except in the presence of a dense and heterogeneous forest stand. As expected, the co-polar and the cross-polar channels are sensitive to different features in the forest. Besides, the reflectivity profiles exhibit a nonlinear dependence of several factors related to forest structure, addressed in the examples proposed in this paper.

The first conclusion is that the tomographic SAR signature is sensitive to the difference of tree species, since analogous spatial distributions with trees of different classes produce different reflectivity profiles. The morphological characteristics of the trees (presence of gaps in the canopy, curved or straight branches, trunk going until the top of the tree or not…) as well as a different phenological cycle (presence or absence of leaves for example) are certainly parameters to be further explored. The second conclusion is that the vertical distribution of the backscatter is also determined by density and by the presence of gaps between the trees, which are parameters characterizing three dimensional forest structure. For example, in the presence of a very dense stand, the highest backscattering is located near the top of the canopy, whereas in a sparser distribution, the peaks in the reflectivity profiles are located at lower heights with respect to the top of the tree. Last, but not least, the importance of the interactions between trees of different types in a stand is also addressed in the paper. For this reason, the interpretation of reflectivity profiles from heterogeneous stands is difficult.

6. References

Capon, J.; “High resolution frequency wavenumber spectrum analysis,” Proc. IEEE, vol. 57, pp 1408-1418, August 1969.

Cloude, S.; Papathanassiou, K. Polarimetric SAR Interferometry, IEEE Transactions of Geosc. and Remote Sens., vol. 36, pp. 1551-1565,1998.

Graham L. C., Synthetic Interferometric Radar for Topographic Mapping, Proc. IEEE, vol. 62, pp. 763-768, June 1974.

Reigber, A.; Moreira, A. First Demonstration of Airborne SAR Tomography Using Multibaseline L-band Data, IEEE Trans. Geosci. Remote Sens., vol. 38, no. 5, pp. 2142-2152, Sep. 2000.

Huang Y., Ferro-Famil L. and Reigber A., “Under foliage object imaging using sar tomography and polarimetric spectral estimators,” Geoscience and Remote Sensing,IEEE Transactions on, 2011.